

From Energy Integration to Photon Counting: Redefining the Design and Performance of Clinical CT

Henrique Carvalho, BS; Peter B. Noël, PhD; Saurabh Jha, MD; Faisal Jamal, MD

Abstract

Computed Tomography (CT) has advanced continuously since the 1970s, evolving from static brain imaging to high-speed, high-resolution volumetric and spectral systems. This review outlines key milestones leading to photon-counting CT (PCCT) and how it addresses the fundamental limitations of energy-integrating detector (EID) technology. While innovations such as helical scanning, multidetector arrays, dual-source systems, and iterative reconstruction (IR) have improved image quality and reduced dose, EID-CT remains constrained by electronic noise, limited spatial resolution, and limited accessibility of spectral information. PCCT introduces direct-conversion detectors that count and classify individual x-ray photons by energy, delivering improved spatial and contrast resolution, intrinsic spectral data, and noise-efficient imaging. PCCT unites ultra-high-resolution, enhanced contrast-to-noise ratio, and multienergy capability in every scan. Early clinical results demonstrate substantial benefits in cardiovascular, pulmonary, musculoskeletal, and oncologic imaging. As PCCT enters routine practice, it marks a paradigm shift toward data-rich, spectrally resolved imaging with greater diagnostic precision and efficiency.

Keywords: photon counting CT, spectral CT, temporal resolution, iodine maps, dual source CT

Introduction

The history of CT is a story of continuous innovation driven by the pursuit of improved diagnostic precision. The journey began in the early 1970s with the pioneering work of Godfrey Hounsfield and Allan Cormack, whose breakthroughs laid the foundation for a technology that would become a cornerstone of modern medical imaging.¹

From those beginnings, CT technology advanced rapidly. Early systems with

narrow fan-beam geometries evolved into wide fan-beam and multidetector-row configurations, enabling greater z-axis coverage and thinner image slices. The introduction of helical (spiral) scanning further improved temporal resolution and scanning efficiency, while refinements in detector design and gantry mechanics enhanced spatial resolution. Concurrently, developments such as automated tube current modulation and IR techniques reduced radiation dose without sacrificing diagnostic accuracy. These

innovations established the framework for modern CT performance and paved the way for emerging technologies.²

Despite these advances, conventional energy-integrating CT still has important limitations. Spatial resolution can be insufficient for coronary CTA in patients with heavy calcification or stents, where blooming and beam-hardening artifacts may obscure fine detail and overestimate stenosis.³ Quantitative accuracy and low-contrast lesion detection may also suffer because Hounsfield Units vary with patient size and surrounding tissue attenuation, and image quality can worsen in larger patients because of reduced dose efficiency and greater electronic noise.⁴

To address some of these challenges, dual-energy CT (DECT) was introduced, allowing material characterization

Affiliations: Herbert Wertheim College of Medicine, Florida International University, Miami, Florida (Carvalho). Perelman School of Medicine at the University of Pennsylvania, Philadelphia, Pennsylvania (Noël, Jha, Jamal).

Disclosures: The authors have no conflicts of interest to disclose. None of the authors received outside funding for the production of this original manuscript and no part of this article has been previously published elsewhere.

through spectral imaging. DECT systems employed methods such as dual x-ray tubes operating at different kilovolt peak (kVp) settings, rapid kVp switching, split-filter techniques, and dual-layer spectral detectors. While DECT represented an important step forward, it continued to rely on EID technology and thus retained some of its inherent constraints.^{4,5}

Recently, PCCT has entered clinical practice as a new approach to x-ray detection. By counting individual photons and recording their energies directly, it offers better spatial and contrast resolution, lower electronic noise, and routine multienergy data from every scan. Together, these features provide a stronger basis for diagnostic performance across a wide range of clinical applications.⁶

Foundations and Early Generations

CT's theoretical basis traces to Johann Radon (1917), who developed the mathematical principles showing that a function can be reconstructed from its line integrals, laying the groundwork for tomographic imaging.⁷ In the 1960s, William Oldendorf built a prototype with a rotating x-ray source and detector that demonstrated cross-sectional imaging.⁸ In parallel, Allan Cormack developed the reconstruction algorithms needed for clinical use.⁹ Building on these foundations, engineer Godfrey Hounsfield designed the first practical CT scanner and, together with James Ambrose, performed the first clinical brain scan in 1971.¹⁰ This marked a turning point in diagnostic medicine and earned Cormack and Hounsfield the 1979 Nobel Prize. This first-generation scanner employed a pencil beam and single detector, requiring several minutes to acquire each slice. Second-generation fan-beam systems (e.g., ACTA, 1973) improved speed, while third-generation rotate-rotate scanners (e.g., Siemens SOMATOM, 1977) achieved whole-body imaging in seconds.

Volumetric Advances

Slip-ring technology eliminated cable constraints, enabling continuous gantry rotation and helical CT in the early 1990s. A slip-ring is an electromechanical device that uses brushes to transmit power and data between a stationary surface and a rotating one, eliminating the need for direct wiring, paving the way for helical (or spiral) CT. In a helical scan, the patient table moves through the continuously rotating gantry, allowing the x-ray beam to trace a spiral trajectory around the body.¹¹ This enabled volumetric imaging within a single breath-hold and facilitated the transition from xenon gas detectors to solid-state technology. These advances produced faster scans, improved image quality, and reduced artifacts.¹¹⁻¹³

Electron Beam CT

Electron beam CT (EBCT) was developed in the 1980s for imaging rapidly moving organs, particularly the heart.¹⁴ Instead of rotating a physical x-ray tube, EBCT employed a stationary anode ring and deflected an electron beam to generate x-rays at multiple points, enabling slice acquisitions in approximately 50-100 ms.^{14,15} This ultrafast temporal resolution made it possible to "freeze" cardiac motion, enabling coronary artery calcium (CAC) scoring and early noninvasive imaging of coronary anatomy.¹⁶ Although EBCT offered superior temporal resolution, it was hampered by lower spatial resolution, limited versatility for body imaging, and high operational cost. Its clinical use declined as ECG-gated multidetector CT (MDCT) emerged.¹⁴

Multidetector, Dual-Source, and Spectral Systems

The late 1990s introduced MDCT, beginning with the Elscint Twin Flash Spiral CT's 2-slice scanner and rapidly

advancing to 16-, 32-, and ultimately 64-slice systems by 2004.¹⁷ The defining feature of MDCT was its capability to capture multiple slices per gantry rotation, significantly expanding volume coverage along the z-axis. Wide-detector arrays enabled near-whole-organ coverage in a single rotation and supported dynamic perfusion imaging of organs such as the brain, heart, and liver.¹⁸ Developments in area-detector technology, exemplified by Canon's Aquilion ONE (introduced in 2007), expanded z-axis coverage to encompass entire organs within one rotation.^{17,19} Contemporary platforms with 256-512 detector rows provide up to 160 mm of coverage, enabling single-beat whole-heart imaging and comprehensive trauma scans in one rotation.²⁰

In 2005, dual-source CT (DSCT) introduced two x-ray tubes and detectors mounted roughly 90° apart, improving temporal resolution relative to single-source MDCT and enabling robust cardiac imaging even at high or irregular heart rates. DSCT also benefits trauma and obese patients by allowing rapid acquisition without sacrificing image quality and offers an alternative to wide-detector scanners.^{21,22} DSCT achieved notable results through shorter acquisition times per view, offering improved resilience to arrhythmias, providing an alternative solution to wide-area coverage, with equal or greater clinical benefits when temporal resolution was the limiting factor.²³

Beyond dual-source systems, rapid kVp-switching and split-filter techniques achieve dual-energy imaging with a single x-ray tube. However, spectral separation is constrained by generator performance and system design, and implementations typically support only a limited set of predefined acquisition protocols. Additionally, rapid kVp switching imposes restrictions on tube current modulation, which limit dose efficiency in large patients.^{4,5}

Dual-layer detector CT uses a single x-ray spectrum combined with a stacked EID design. The top scintillator layer

absorbs lower-energy photons, while higher-energy photons penetrate to the lower layer. Because spectral separation occurs at the detector rather than the source, dual-layer CT intrinsically acquires spectral data for every scan without requiring protocol selection. However, spectral separation is constrained by the physics of scintillator absorption, resulting in greater overlap between the energy spectra than in source-based dual-energy. This overlap is mitigated using advanced reconstruction algorithms and deep-learning techniques.^{4,24} This transformed CT from a purely anatomic modality into one that also integrates tissue characterization and functional insights.^{25,26} Despite these innovations, performance remained constrained by the fundamental limitations of energy-integrating detectors.^{27,28}

Iterative Reconstruction

Filtered back projection (FBP) has been the standard analytic method for CT reconstruction, applying a filter to projection data and back-projecting the result to form images. The filtering step corrects the blurring inherent in simple back-projection, and the overall process is efficient. However, FBP is prone to increased noise and streak artifacts with reduced radiation dose or undersampled projection data. These shortcomings prompted the development of more advanced reconstruction methods.²⁹⁻³¹

IR algorithms address the limitations of FBP for applications requiring dose reduction. IR methods start with an initial image estimate and iteratively refine it by comparing it to the measured data. This process allows selective suppression of noise and artifact reduction, enabling radiation reduction while maintaining or improving image quality. However, IR can introduce unnatural image textures and is computationally more demanding than FBP, which has limited its universal adoption.^{27,32,33}

In both DECT and PCCT, IR improves image quality and quantitative reliability under challenging noise and spectral conditions by more accurately modeling polychromatic spectra, detector response, and statistical noise. This facilitates more robust material decomposition and helps translate spectral data into clinically usable images, such as low-noise virtual monoenergetic images (VMIs) and quantitative maps at doses comparable to conventional CT.^{27,33}

Deep learning image reconstruction (DLIR) utilizes convolutional neural networks to produce images with reduced noise and preserved anatomical detail, while maintaining a noise texture comparable to that of FBP. DLIR enables more radiation dose reduction without compromising diagnostic accuracy or low-contrast detectability. However, DLIR performance depends on the quality of training data and continued validation across a broad range of clinical applications.³⁴⁻³⁶

Introduction of Photon-Counting Detectors

PCCT has evolved through decades of innovation and translational research. In the early 2000s, General Electric (GE) conducted the first human scan using a prototype system, while Philips introduced the first rotating-gantry PCCT designed for small animal imaging, generating preclinical data.^{28,37,38} By the 2010s, both Siemens and Philips had developed advanced prototypes capable of whole-body imaging and spectral acquisition, enabling preclinical and early human research. This progress culminated in 2021 with Siemens' introduction of the first full-field-of-view clinical PCCT system, soon followed by platforms from other vendors (GE, Canon, United Imaging). The transition from research to clinical practice enabled large-scale studies confirming PCCT's advantages in spatial resolution, spectral imaging, and artifact reduction.^{28,39-41}

The difference between conventional and PCCT lies in the detector design. Traditional EID-CT systems use an indirect, two-step process. First, x-ray photons strike a scintillator that converts their energy into visible light photons. These photons travel to a photodiode, converting them into a cumulative electrical signal (see Figure 1). One drawback is that the light conversion results in loss of the spectral identity of individual x-ray photons. Furthermore, the light produced by the scintillator tends to scatter, necessitating physical septa-light-blocking dividers that isolate individual detector pixels and prevent optical crosstalk. The space occupied by these septa represents a "dead area" insensitive to x-rays, reducing the detector's geometric dose efficiency, particularly as pixel size decreases.^{38,42}

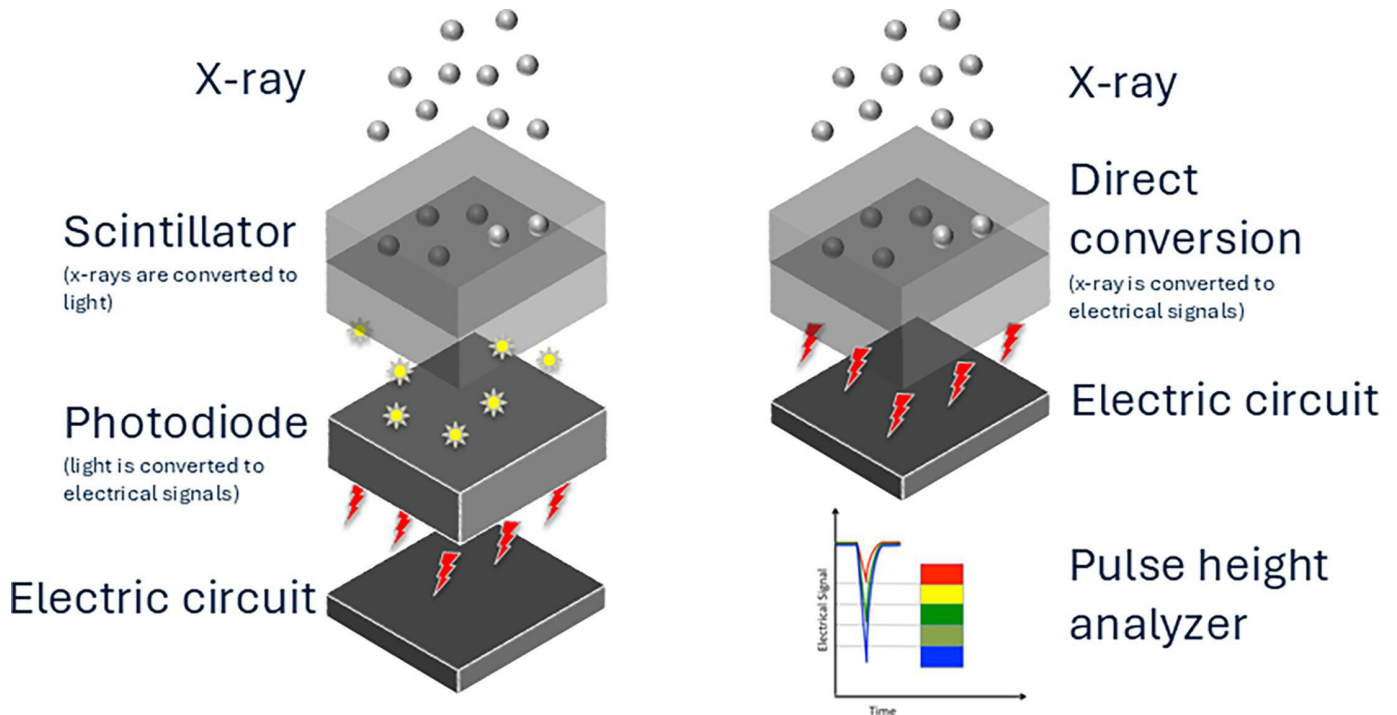
In contrast (see Figure 1), PCCT uses a direct, single-step conversion process. The detector is made of high-atomic-number semiconductor materials such as cadmium telluride (CdTe), cadmium zinc telluride (CZT), or silicon (Si), which are efficient absorbers of x-rays.^{38,42-44} When an x-ray photon strikes the semiconductor, it generates electron-hole pairs directly within the detector material. An electric field separates these pairs, driving the electrons toward a positively charged, pixelated anode, creating a short electrical pulse. The height of this voltage pulse is directly proportional to the energy of the absorbed photon. An application-specific integrated circuit (ASIC) captures each pulse, categorizing them into discrete energy bins according to preselected thresholds (see Figure 2). This direct detection and energy-sorting mechanism is the foundation for all the key advantages of PCD-CT.^{38,42,44,45}

Key Technical Advancements and Their Synergistic Effects

High Spatial Resolution

PCDs eliminate the need for physical septa because the signal is generated electronically rather than optically,

Figure 1. Comparison of energy-integrating detector (EID) and photon-counting detector architectures. Left: conventional EID-CT uses a 2-step, indirect conversion process in which x-ray photons are first absorbed by a scintillator that converts them into visible light. The resulting light photons are then detected by a photodiode and converted into electrical signals. This indirect process causes light scatter and loss of spectral information. Right: In photon-counting CT (PCCT), x-ray photons are directly converted into electrical signals within a semiconductor layer, eliminating the scintillator. Each photon is individually counted and its energy measured by a pulse height analyzer, enabling direct energy discrimination and multienergy data acquisition from a single scan.



allowing smaller detector pixels without sacrificing geometric detection efficiency. The result is a substantial increase in spatial resolution, enabling ultra-high-resolution (UHR) imaging with a single slice thickness as thin as 0.2 mm. For comparison, typical EID-CT detector pixel sizes range from 0.5 to 0.625 mm, achieving measured in-plane resolutions of 20–25 line pairs per centimeter (lp/cm) (10% MTF) with sharp kernels. As stated, PCCT detectors use subpixel binning ($0.151 \times 0.176 \text{ mm}^2$ at isocenter unbinned; $0.302 \times 0.352 \text{ mm}^2$ binned), enabling UHR modes with limiting resolutions of 40 lp/cm (125 μm) or finer. Reconstruction kernels affect realized resolution: standard kernels yield equivalent MTF curves across detector sizes (~ 10 lp/cm), while ultra-sharp kernels unlock PCCT's full potential, achieving 16–18 lp/cm (10% MTF) versus ~ 9 –10 lp/cm for EID-CT.^{39,46,47} This improved spatial resolution is

essential for visualizing fine anatomic structures and can be achieved without the dose penalty often associated with high-resolution modes on conventional CT systems.⁴⁸

Noise Elimination and Enhanced Contrast

Another advantage of PCCT is its ability to eliminate electronic noise.⁴⁹ The lowest energy threshold in the detector's counting process can be set to a level above the energy of pulses caused by electronic noise.⁴⁵ By filtering out low-energy photons, PCD-CT's signal contains primarily statistical quantum noise, resulting in lower-noise images, especially under low x-ray flux conditions. This is beneficial for low-dose CT protocols and for imaging obese patients.⁴⁵ Clinical studies report noise reductions of approximately 40% in PCCT compared with EID-CT at matched radiation

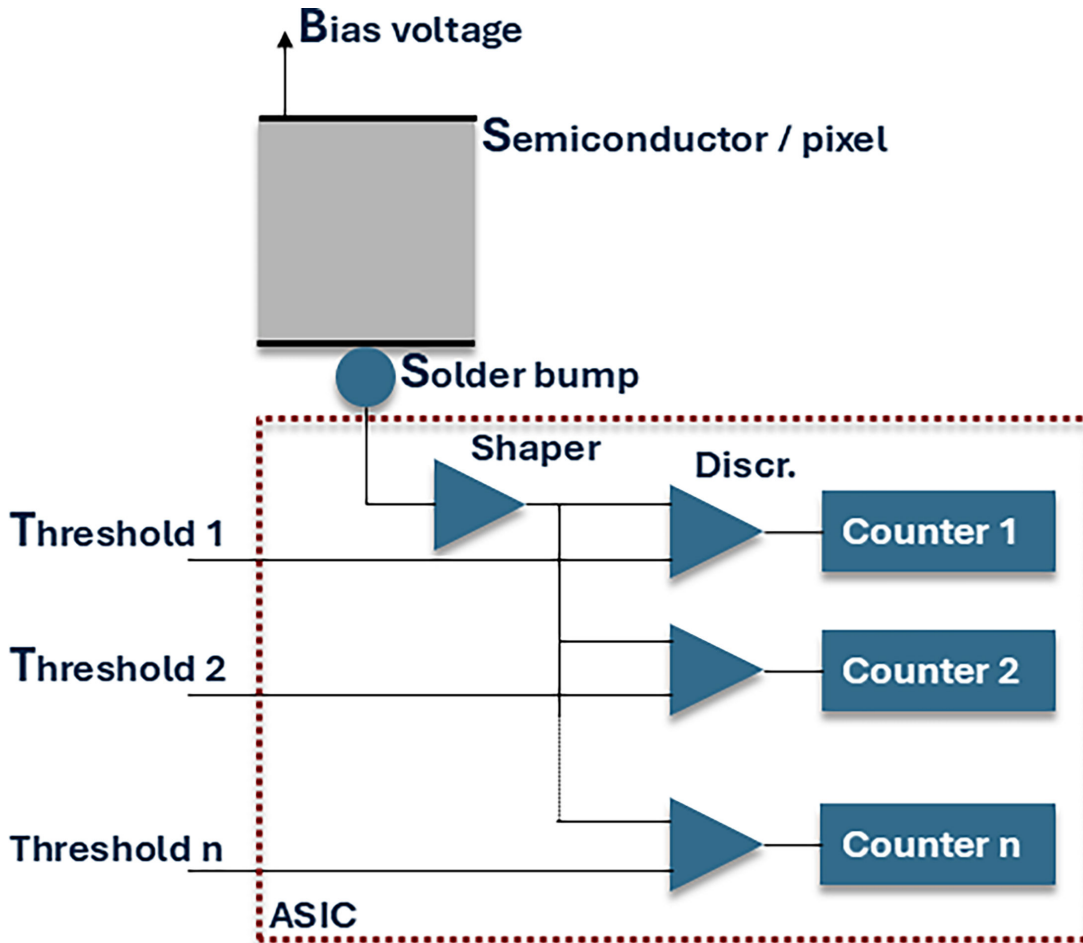
dose,⁵⁰ or radiation dose reductions of approximately 20–30% while maintaining equivalent noise levels.^{28,51}

Furthermore, the direct conversion approach gives equal weight to all detected photons. This is a change from EID-CT, where lower-energy photons contribute less to the final signal. Since low-energy x-rays are more likely to be attenuated by materials like iodine, this equal weighting enhances the contribution of these photons, resulting in a higher CNR and improved soft-tissue contrast.⁴⁵

Multienergy and Spectral Imaging

Another feature of PCCT is its inherent ability to acquire multi-energy spectral information. The detector's ASIC sorts photons into energy bins based on their deposited energy. This capability is inherently acquired, ensuring that spectral information is acquired for every scan without the need for a protocol

Figure 2. Schematic of a photon-counting detector pixel architecture. Each pixel consists of a semiconductor sensor connected to an application-specific integrated circuit (ASIC) via a solder bump. When x-ray photons interact with the semiconductor, they generate electrical pulses that are shaped and processed by the ASIC. The signal passes through multiple energy thresholds, each linked to a discriminator and a corresponding counter. This configuration allows the detector to sort and count individual photons according to their energy levels, enabling simultaneous multi-energy data acquisition for spectral CT imaging.



or prospective selection, as is often the case with EID-based rapid kVp switching, split-filter methods, and dual-source systems. This allows for retrospective reconstruction of advanced image types, including VMIs, virtual noncontrast (VNC) images, iodine maps, and other material-specific reconstructions.⁵²

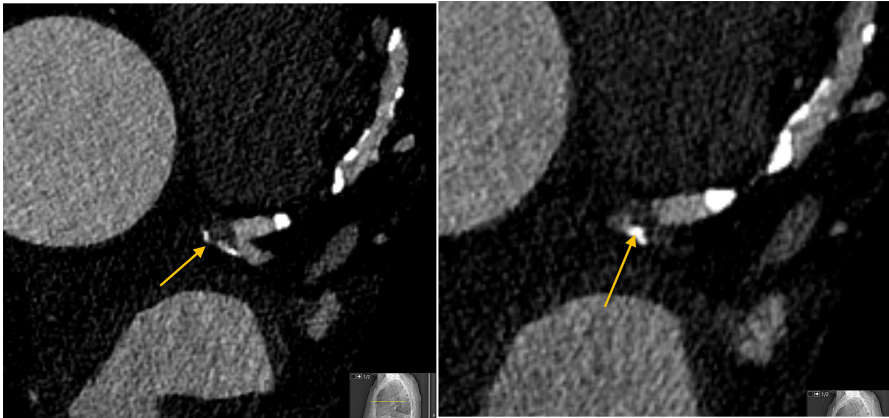
Quantitative assessment of spectral CT performance relies on spectral separation, iodine-related contrast-to-noise ratio (CNR), iodine quantification bias, and the effectiveness of iodine suppression in VNC images. In clinical PCCT, VNC quality is evaluated by comparing

attenuation in VNC reconstructions with true noncontrast images; for example, aortic valve calcium studies with dual-source PCCT have reported that the fraction of cardiac voxels above 130 HU is reduced from roughly 80% in contrast-enhanced CTA to about 0.2–0.6% in PCCT-derived VNC series, closely matching values of approximately 0.5–1% in true noncontrast scans and indicating near-complete suppression of iodine-related signal. Phantom studies of PCCT further show iodine quantification errors on the order of a few milligrams per milliliter (mg/mL) and percentage

biases within low single digits across a range of iodine concentrations and dose levels, supporting its use as a quantitatively robust platform for VNC, iodine maps, and virtual monoenergetic imaging.^{53–56}

For iodine maps, performance is characterized by iodine concentration error (mg/mL), percentage bias, and measurement precision across repeated acquisitions. Phantom experiments with clinical PCCT systems demonstrated small absolute iodine errors and low percentage bias, often within low single digits over clinically relevant concentration ranges and down to reduced dose

Figure 3. Photon-counting CT reduces blooming artifact from coronary calcium. Photon-counting detector CT with ultra-high-resolution acquisition (left, 0.2 mm ultra-high-resolution [UHR], Bv56u kernel) depicts distal left main bifurcation plaque with sharply defined calcified components and preserved visualization of the true lumen extending into the proximal left anterior descending and left circumflex arteries, minimizing calcium blooming. In contrast, a standard-resolution photon-counting detector CT acquisition without UHR mode (right) demonstrates more pronounced blooming of the same calcified plaque, obscuring the residual lumen and leading to overestimation of stenosis severity and potential up-classification of Coronary Artery Disease-Reporting and Data System (CAD-RADS).



levels, indicating accurate and dose-stable iodine quantification. VMIs are evaluated using iodine CNR, noise, and HU accuracy as functions of energy, and PCCT studies show that low-keV VMIs (around 40–60 keV) can provide increased iodine CNR while maintaining noise characteristics compatible with quantitative use, supporting PCCT as a robust platform for quantitative spectral imaging.⁵⁵⁻⁵⁸

Clinical Applications

Technical enhancements of PCCT translate into clinical benefits across a wide spectrum of radiological subspecialties. In cardiovascular imaging, high spatial and temporal resolution and advanced artifact reduction techniques address the “triple threat” of motion, calcification, and stents, leading to more accurate stenosis assessment and a reduction in obscuring artifacts⁵⁹ (Figure 3). Reduction in stenosis degree often leads to reclassification rate to a lower CAD-RADS with PCD-CT, one study demonstrating a 49% rate of reclassification.⁶⁰ In ILD, ultra-high-resolution PCCT improved depiction of fine fibrotic changes, increasing the median visible bronchial generation from the 9th to the 10th order and raising the

proportion of clearly delineated bronchial walls from 23% to 57%, while reducing CT DIvol and DLP by approximately 27% and 32%, respectively, and reclassifying 4/112 patients from non-fibrotic to fibrotic ILD.⁶¹ In oncology, PCCT enhances detection of skull base infiltration, laryngeal cartilage involvement, and small pulmonary nodules through superior spatial resolution. Spectral capabilities provide higher iodine CNR in low-keV VMIs for improved lesion conspicuity and achieve 94% sensitivity for hepatic steatosis detection using VNC images. High-resolution imaging of trabecular bone microstructure improves visualization and characterization of osseous metastases.⁶² PCCT is poised to usher in new diagnostic paradigms, from quantitative data extraction during routine screening to functional imaging enabled by next-generation contrast agents.⁶³

Overcoming Technical Hurdles

PCCT's clinical adoption has required continued efforts to address several intrinsic physical challenges. Key issues include charge sharing, when a photon's charge cloud spreads across adjacent pixels and is registered at lower energies, and K-escape, when detector interactions generate secondary fluorescence that

can be absorbed by neighboring pixels. Both can reduce energy discrimination accuracy, but modern systems mitigate these effects through smaller pixel sizes and coincidence logic that combines simultaneous signals into a single count.^{28,64}

Pulse pile-up is another limitation, occurring when individual photon pulses overlap at very high x-ray flux and are registered as one event, which underestimates photon count and overestimates photon energy. It can be partially corrected with calibration-based algorithms, but is best limited by high-speed readout electronics and detector pixel optimization.^{28,64}

From a clinical standpoint, most charge-sharing and pile-up corrections are handled by scanner hardware and reconstruction software. Only extreme high-flux protocols, such as very high tube current cardiac imaging, may require additional protocol optimization, while routine practice is usually managed by automated flux control, optimized pixel sizing, and calibration-based corrections. These limitations therefore rarely affect day-to-day radiologist workflow, though they remain important for understanding scanner behavior at the extremes of dose and temporal resolution.

Conclusion

Over more than five decades, CT has evolved from rudimentary brain imaging to high-speed, high-resolution volumetric and spectral systems. Each innovation, from helical scanning and multidetector CT to dual-source geometries and iterative reconstruction, incrementally improved diagnostic confidence. PCCT represents a transformative step forward in computed tomography, moving beyond the limitations of conventional energy-integrating detector systems. By directly counting individual x-ray photons, this technology delivers a host of synergistic benefits, including unprecedented spatial resolution, the virtual elimination of electronic noise, and the intrinsic spectral data from every scan.

These technical advantages are directly translating today into improved diagnostic capabilities across a range of clinical applications, from cardiovascular and musculoskeletal imaging to oncology and pediatric radiology. The shift to PCCT is poised to enhance diagnostic confidence, streamline workflows, and create new opportunities for earlier disease detection and improved management. This transition, from protocol-driven to data-rich imaging, marks the next era in the ongoing evolution of CT technology.

References

- Hounsfield GN. Computed medical imaging. *Science*. 1980;210(4465):22-28. doi:10.1126/science.6997993
- Kalender WA. *Computed Tomography: Fundamentals, System Technology, Image Quality, Applications*. Publicis Publishing; 2011.
- Sun Z, Choo GH, Ng KH. Coronary CT angiography: current status and continuing challenges. *Br J Radiol*. 2012;85(1013):495-510. doi:10.1259/bjr/15296170
- McCollough CH, Leng S, Yu L, Fletcher JG. Dual- and multi-energy CT: principles, technical approaches, and clinical applications. *Radiology*. 2015;276(3):637-653. doi:10.1148/radiol.2015142631
- Sellerer T, Noël PB, Patino M, et al. Dual-energy CT: a phantom comparison of different platforms for abdominal imaging. *Eur Radiol*. 2018;28(7):2745-2755. doi:10.1007/s00330-017-5238-5
- Taguchi K, Iwanczyk JS. Vision 20/20: single photon counting x-ray detectors in medical imaging. *Med Phys*. 2013;40(10):100901. doi:10.1118/1.4820371
- Radon J. On the determination of functions from their integral values along certain manifolds. *IEEE Trans Med Imaging*. 1986;5(4):170-176. doi:10.1109/TMI.1986.4307775
- Oldendorf WH. Isolated flying spot detection of radiodensity discontinuities—displaying the internal structural pattern of a complex object. *IRE Trans Bio-med Electron*. 1961;8(1):68-72. doi:10.1109/TBME.1961.4322854
- Cormack AM. Representation of a function by its line integrals, with some radiological applications. *J Appl Phys*. 1963;34(9):2722-2727. doi:10.1063/1.1729798
- Hounsfield GN. Computerized transverse axial scanning (tomography). Part 1. Description of system. *Br J Radiol*. 1973;46(552):1016-1022. doi:10.1259/0007-1285-46-552-1016
- Flohr T. CT systems. *Curr Radiol Rep*. 2013;1(1):52-63. doi:10.1007/s40134-012-0005-5
- Zenger I. *The History of Computed Tomography at Siemens Healthineers*. Siemens Healthcare GmbH; 2021.
- Fuchs T, Kachelriess M, Kalender WA. Direct comparison of a xenon and a solid-state CT detector system: measurements under working conditions. *IEEE Trans Med Imaging*. 2000;19(9):941-948. doi:10.1109/42.887841
- Kulkarni S, Rumberger JA, Jha S. Electron beam CT: a historical review. *AJR Am J Roentgenol*. 2021;216(5):1222-1228. doi:10.2214/AJR.19.22681
- Mittal TK, Rubens MB. Computed tomography techniques and principles. part a. electron beam computed tomography. In: Anagnostopoulos CD, Nihoyannopoulos P, Bax JJ, Wall E, eds. *Noninvasive Imaging of Myocardial Ischemia*. Springer London. 2006:93-98. doi:10.1007/1-84628-156-3_6
- Arad Y, Spadaro LA, Goodman K, et al. Predictive value of electron beam computed tomography of the coronary arteries. 19-month follow-up of 1173 asymptomatic subjects. *Circulation*. 1996;93(11):1951-1953. doi:10.1161/01.cir.93.11.1951
- Kohl G. The evolution and state-of-the-art principles of multislice computed tomography. *Proc Am Thorac Soc*. 2005;2(6):470-476. doi:10.1513/pats.200508-086DS
- Mori S, Endo M, Tsunoo T, et al. Physical performance evaluation of a 256-slice CT-scanner for four-dimensional imaging. *Med Phys*. 2004;31(6):1348-1356. doi:10.1118/1.1747758
- Toshiba. Toshiba launches breakthrough CT system—the Aquilion ONE; 2007. <https://us.medical.canon/news/press-releases/2007/11/26/252/>
- GE H. GoldSeal™ Revolution™ CT EX 160 mm. https://www.gehealthcare.com/-/jssmedia/gehc/us/images/products/goldseal/goldseal-ct-redesign/sell-sheet-goldseal-revolution-ct-ex160-us-jb02387xx_v2.pdf?rev=-1&srsltid=AfmBOophfUbd95WwMBJAfFQJWzbLl2VxMZGiB-socPjh0QM6KVjgnGDHT
- Flohr TG, McCollough CH, Bruder H, et al. First performance evaluation of a dual-source CT (DSCT) system. *Eur Radiol*. 2006;16(2):256-268. doi:10.1007/s00330-005-2919-2
- Achenbach S, Ropers D, Kuettner A, et al. Contrast-enhanced coronary artery visualization by dual-source computed tomography—initial experience. *Eur J Radiol*. 2006;57(3):331-335. doi:10.1016/j.ejrad.2005.12.017
- Achenbach S, Marwan M, Ropers D, et al. Coronary computed tomography angiography with a consistent dose below 1 msv using prospectively electrocardiogram-triggered high-pitch spiral acquisition. *Eur Heart J*. 2010;31(3):340-346. doi:10.1093/eurheartj/ehp470
- Johnson TRC, Krauss B, Sedlmair M, et al. Material differentiation by dual energy CT: initial experience. *Eur Radiol*. 2007;17(6):1510-1517. doi:10.1007/s00330-006-0517-6
- Hokamp NG, Maintz D, Shapira N, et al. Technical background of a novel detector-based approach to dual-energy computed tomography. *Diagn Interv Radiol Ank Turk*. 2020;26(1):68-71. doi:10.5152/dir.2019.19136
- Philips. Philips launches world's first detector-based spectral CT scanner in Canada; 2016. <https://www.usa.philips.com/a-w/about/news/archive/standard/news/press/2016/20161115-Philips-launches-first-spectral-ct-scanner-in-canada.html>
- Geyer LL, Schoepf UJ, Meinel FG, et al. State of the art: iterative CT reconstruction techniques. *Radiology*. 2015;276(2):339-357. doi:10.1148/radiol.2015132766
- Willeminck MJ, Persson M, Pourmorteza A, Pelc NJ, Fleischmann D. Photon-counting CT: technical principles and clinical prospects. *Radiology*. 2018;289(2):293-312. doi:10.1148/radiol.2018172656
- Koetzier LR, Mastrodicasa D, Szczykutowicz TP, et al. Deep learning image reconstruction for CT: technical principles and clinical prospects. *Radiology*. 2023;306(3):e221257. doi:10.1148/radiol.221257
- Schofield R, King L, Tayal U, et al. Image reconstruction: part 1 - understanding filtered back projection, noise and image acquisition. *J Cardiovasc Comput Tomogr*. 2020;14(3):219-225. doi:10.1016/j.jcct.2019.04.008
- Shi H, Luo S, Yang Z, Wu G. A novel iterative CT reconstruction approach based on FBP algorithm. *PLoS One*. 2015;10(9):e0138498. doi:10.1371/journal.pone.0138498
- Guido G, Polici M, Nacci I, et al. Iterative reconstruction: state-of-the-art and future perspectives. *J Comput Assist Tomogr*. 2023;47(2):244-254. doi:10.1097/RCT.0000000000001401
- Willeminck MJ, de Jong PA, Leiner T, et al. Iterative reconstruction techniques for computed tomography part 1: technical principles. *Eur Radiol*. 2013;23(6):1623-1631. doi:10.1007/s00330-012-2765-y
- Chandran M O, Pendem S, Priya PS, et al. Comparison of image quality between deep learning image reconstruction and iterative reconstruction technique for CT brain - a pilot study. *F1000Res*. 2024;13:691. doi:10.12688/f1000research.150773.1
- Bornet P-A, Villani N, Gillet R, et al. Clinical acceptance of deep learning reconstruction for abdominal CT imaging: objective and subjective image quality and low-contrast detectability assessment. *Eur Radiol*. 2022;32(5):3161-3172. doi:10.1007/s00330-021-08410-x

- 36) Willeminck MJ, Noël PB. The evolution of image reconstruction for CT-from filtered back projection to artificial intelligence. *Eur Radiol.* 2019;29(5):2185-2195. doi:10.1007/s00330-018-5810-7
- 37) McCollough CH, Rajiah PS. Milestones in CT: past, present, and future. *Radiology.* 2023;309(1):e230803. doi:10.1148/radiol.230803
- 38) Leng S, Bruesewitz M, Tao S, et al. Photon-counting detector CT: system design and clinical applications of an emerging technology. *Radiographics.* 2019;39(3):729-743. doi:10.1148/rg.2019180115
- 39) Sartoretto T, Wildberger JE, Flohr T, Alkadhi H. Photon-counting detector CT: early clinical experience review. *Br J Radiol.* 2023;96(1147):20220544. doi:10.1259/bjr.20220544
- 40) Alkadhi H, Runge V. The future arrived: photon-counting detector CT. *Invest Radiol.* 2023;58(7):439-440. doi:10.1097/RLI.0000000000000985
- 41) Schwartz FR, Sodickson AD, Pickhardt PJ, et al. Photon-counting CT: technology, current and potential future clinical applications, and overview of approved systems and those in various stages of research and development. *Radiology.* 2025;314(3):e240662. doi:10.1148/radiol.240662
- 42) Schwartz FR, Dane B, Su S, et al. Getting started with photon-counting CT: optimizing your setup for success. *Radiographics.* 2025;45(2):e240106. doi:10.1148/rg.240106
- 43) GE H. Silicon dreams: a technological breakthrough to let doctors peer inside the body with startling clarity; 2022. <https://www.gehealthcare.com/insights/article/silicon-dreams-a-technological-breakthrough-to-let-doctors-peer-inside-the-body-with-startling-clarity?srsltid=AfmBOooXMC7cZaYHwKMC3wIRNPxR9dg5VLBTtqBF0Jovg6pIImeEFH0U>
- 44) Abbaspour S, Mahmoudian B, Islamian JP. Cadmium telluride semiconductor detector for improved spatial and energy resolution radioisotopic imaging. *World J Nucl Med.* 2017;16(2):101-107. doi:10.4103/1450-1147.203079
- 45) Hsieh SS, Leng S, Rajendran K, Tao S, McCollough CH. Photon counting CT: clinical applications and future developments. *IEEE Trans Radiat Plasma Med Sci.* 2021;5(4):441-452. doi:10.1109/trpms.2020.3020212
- 46) Zhou W, Lane JI, Carlson ML, et al. Comparison of a photon-counting-detector CT with an energy-integrating-detector CT for temporal bone imaging: a cadaveric study. *AJNR Am J Neuroradiol.* 2018;39(9):1733-1738. doi:10.3174/ajnr.A5768
- 47) Leng S, Rajendran K, Gong H, et al. 150- μ m spatial resolution using photon-counting detector computed tomography technology: technical performance and first patient images. *Invest Radiol.* 2018;53(11):655-662. doi:10.1097/RLI.0000000000000488
- 48) Esquivel A, Ferrero A, Mileto A, et al. Photon-counting detector CT: key points radiologists should know. *Korean J Radiol.* 2022;23(9):854-865. doi:10.3348/kjr.2022.0377
- 49) Liu LP, Shapira N, Chen AA, et al. First-generation clinical dual-source photon-counting CT: ultra-low-dose quantitative spectral imaging. *Eur Radiol.* 2022;32(12):8579-8587. doi:10.1007/s00330-022-08933-x
- 50) Rajendran K, Petersilka M, Henning A, et al. First clinical photon-counting detector CT system: technical evaluation. *Radiology.* 2022;303(1):130-138. doi:10.1148/radiol.212579
- 51) Rajagopal JR, Farhadi F, Solomon J, et al. Comparison of low dose performance of photon-counting and energy integrating CT. *Acad Radiol.* 2021;28(12):1754-1760. doi:10.1016/j.acra.2020.07.033
- 52) Flohr T, Schmidt B. Technical basics and clinical benefits of photon-counting CT. *Invest Radiol.* 2023;58(7):441-450. doi:10.1097/RLI.0000000000000980
- 53) Risch F, Harmel E, Rippel K, et al. Virtual non-contrast series of photon-counting detector computed tomography angiography for aortic valve calcium scoring. *Int J Cardiovasc Imaging.* 2024;40(4):723-732. doi:10.1007/s10554-023-03040-4
- 54) McCollough CH, Rajendran K, Leng S. Standardization and quantitative imaging with photon-counting detector CT. *Invest Radiol.* 2023;58(7):451-458. doi:10.1097/RLI.0000000000000948
- 55) Tao A, Huang R, Tao S, et al. Dual-source photon counting detector CT with a tin filter: a phantom study on iodine quantification performance. *Phys Med Biol.* 2019;64(11):115019. doi:10.1088/1361-6560/ab1c34
- 56) Winfree T, Treb K, McCollough C, Leng S. Spectral performance for iodine quantification of a dual-source, dual-kV photon counting detector CT. *Med Phys.* 2025;52(5):2824-2831. doi:10.1002/mp.17679
- 57) Vrbaski S, Bache S, Rajagopal J, Samei E. Quantitative performance of photon-counting CT at low dose: virtual monochromatic imaging and iodine quantification. *Med Phys.* 2023;50(9):5421-5433. doi:10.1002/mp.16583
- 58) Cester D, Eberhard M, Alkadhi H, Euler A. Virtual monoenergetic images from dual-energy CT: systematic assessment of task-based image quality performance. *Quant Imaging Med Surg.* 2022;12(1):726-741. doi:10.21037/qims-21-477
- 59) Si-Mohamed SA, Boccalini S, Lacombe H, et al. Coronary CT angiography with photon-counting CT: first-in-human results. *Radiology.* 2022;303(2):303-313. doi:10.1148/radiol.211780
- 60) Vecsey-Nagy M, Tremamunno G, Schoepf UJ, et al. Intraindividual comparison of ultrahigh-spatial-resolution photon-counting detector CT and energy-integrating detector CT for coronary stenosis measurement. *Circ Cardiovasc Imaging.* 2024;17(10):e017112. doi:10.1161/CIRCIMAGING.124.017112
- 61) Gaillandre Y, Duhamel A, Flohr T, et al. Ultra-high resolution CT imaging of interstitial lung disease: impact of photon-counting CT in 112 patients. *Eur Radiol.* 2023;33(8):5528-5539. doi:10.1007/s00330-023-09616-x
- 62) Hagen F, Soschynski M, Weis M, et al. Photon-counting computed tomography - clinical application in oncological, cardiovascular, and pediatric radiology. *Rofo.* 2024;196(1):25-35. doi:10.1055/a-2119-5802
- 63) Hsu JC, Nieves LM, Betzer O, et al. Nanoparticle contrast agents for x-ray imaging applications. *Wiley Interdiscip Rev Nanomed Nanobiotechnol.* 2020;12(6):e1642. doi:10.1002/wnan.1642
- 64) Nakamura Y, Higaki T, Kondo S, et al. An introduction to photon-counting detector CT (PCD CT) for radiologists. *Jpn J Radiol.* 2023;41(3):266-282. doi:10.1007/s11604-022-01350-6